Flow Control for Rotorcraft Applications at Flight Mach Numbers

Hassan NAGIB, John KIEDAISCH

Illinois Institute of Technology, Chicago, IL USA

David GREENBLATT

TU Berlin, Berlin, Germany

Israel WYGNANSKI

University of Arizona, Tuscon, AZ, USA

Ahmed HASSAN

The Boeing Company, Mesa, AZ, USA

Abstract. Pulsating zero-mass flux jets introduced from spanwise slots at various locations on the upper surface of oscillating VR-7 and VR-22 airfoil models are shown to be effective in controlling lift, moment and drag coefficients over the range of Mach numbers from 0.1 to 0.4. This control is demonstrated over a wide range of mean angles of attack of the oscillating airfoil from light to deep stall conditions. Maintaining the non-dimensional frequency and amplitude of the forcing unchanged results in comparable modifications of the aerodynamic coefficients throughout this Mach number range, even in presence of local shocks. Therefore, it appears that this active-flow control technique is only limited by the ability to generate the adequate forcing conditions at the higher Mach numbers required for applications such as rotorcraft.

Key words: active flow control, oscillating airfoil, unsteady, compressible

1. Introduction

In modern design of military or high-performance aircraft, separation control is vital to improving the flight characteristics of airfoils whether the application is highly maneuverable fighters, stealth bombers, long-endurance flight or micro air vehicles. When air separates from a wing in flight, the result is loss of lift and increase in drag that threatens the stability of the aircraft and the safety of the pilot. Separation is typically avoided by geometric changes and by flying the aircraft within the flight envelope. Recently, periodic excitation (or forcing) has been demonstrated as an effective, efficient and practical method for controlling incompressible dynamic stall (e.g. Greenblatt & Wygnanski)[1]. Based on these results it is obvious to expect that the technique may also be effective in improving the performance of a wide range of airfoils used in the rotorcraft industry such as those carefully documented by McAlister et al.[2]. However, Carr[5] concludes that compressibility can have a profound effect on dynamic stall, even at relatively moderate Mach numbers, i.e.

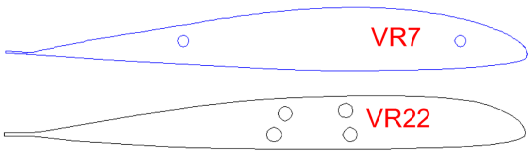

Figure 1. VR-7 and VR-22 airfoil cross-sections.

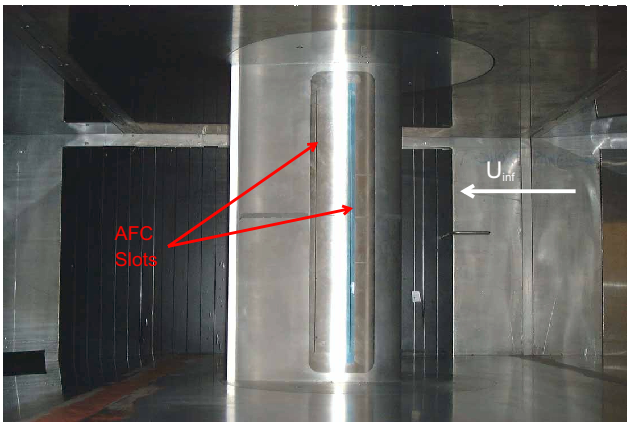

Figure 2. VR-7 airfoil model installed in the NDF test section.

$M = 0.3$, when the flow can be supersonic in the leading-edge region. Although in Carr's case the airfoil stall was dominated by leading edge separation, where compressibility effects may be exaggerated by a shock/boundary layer interaction, Carr and Chandrasekhara[6] projected that such effects would lead to the failure of flow control methodologies in all unsteady airfoil applications for Mach numbers equal to or larger than about 0.3. When attempting dynamic stall control, compressibility must be seriously considered because typical full-scale Mach numbers on a rotorcraft retreating blade in the vicinity of dynamic stall are in the range from 0.3 to 0.5. We should point out that, apparently, the effect of Reynolds number is less understood due to the difficulty of varying Reynolds number significantly without introducing compressibility effects.

2. Objectives and Experimental Setup

The global objective of this work was to study the effectiveness of periodic forcing on the control of rotorcraft dynamic stall at typical flight Mach numbers. It is well known that significant changes in the characteristics of stall occur due to compressibility for $M > 0.3$. The experimental data presented here, based on surface pressure measurements and wake velocity surveys for drag estimates, will summarize a detailed investigation carried out in the NDF at IIT using $M = 0.3$, 0.35, and 0.4. Either one of two models of VR-7 and VR-22 airfoils (Fig. 1) with a 0.36 m chord and 0.56 m span was mounted vertically in the NDF test section during the tests. The airfoils could be dynamically pitched about their quarter-chord location through $\pm 15^o$ with mean angles ranging from 0^o to $\pm 15^o$. The airfoils were tested in the National Diagnostic Facility at IIT (see Figs. 2 and 3), and more details of the

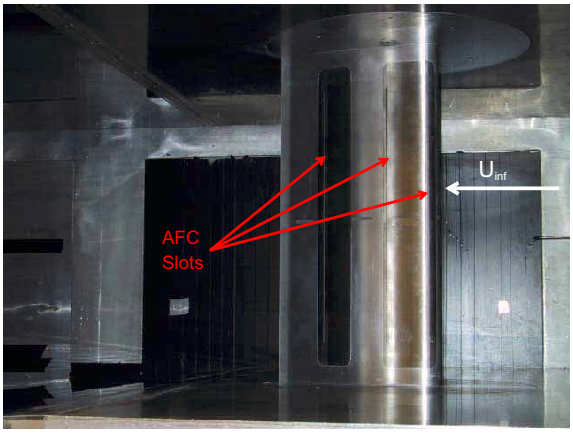

Figure 3. VR-22 airfoil model installed in the NDF test section.

setup and techniques used can be found in Greenblatt et al.[3] and Nagib et al.[4]. The airfoils were equipped with 44 static pressure ports around their perimeter.

3. Results

The VR-7 results compared favorably with the classical data of Mcalister et al.[2] providing confirmation of our data processing scheme[3]. Figures 4, 5, 6, and 7 display sample data showing the effect of varying the mean incidence angle at $M = 0.3$, while maintaining incidence angle excursions of 5^o, for baseline (Figs. 4 and 5) and controlled (Figs. 6 and 7) scenarios (all values of C_L, C_M, C_μ and F^+ are provided here in relative magnitude.) These data, summarize and confirm the effectiveness of this control technique over a wide range of angles, from light stall conditions well into deep stall. For the light-stall scenario, it was clearly seen[4] that the increase in M has no deleterious effect whatsoever on the effectiveness of forcing. In fact, the negative moment, relative to the baseline value, introduced at $M = 0.1$ under these forcing conditions is somewhat alleviated with increasing Mach number. Therefore, while the effectiveness of forcing certainly does not diminish, there is evidence to suggest that it may be superior at the higher Mach numbers. The sample chordwise pressure distributions shown in Figs. 8 and 9 demonstrate that a supercritical flow region is present near the leading edge of the VR-7 airfoil during pitch-up. This region was observed in the baseline pressure distributions over a range of α, and this range increased with increasing Mach number. At lower Mach numbers, it was observed that at some α's, where the baseline flow was not supercritical, the flow in the leading-edge region became supercritical in the presence of AFC reflecting the decrease in separation. At higher Mach numbers, the effect of AFC did not diminish at α's where the baseline flow was already supercritical.
Figures 10 and 11 show a similar comparison to that presented by Nagib et al.[4], with the exceptions that the airfoil is moved far into the post-stall regime (with maximum incidence angle 10^o beyond the static stall angle) and a different forcing frequency is used. Here, both lift and moment stall are severe. Introducing and increasing the forcing amplitude has the effect of increasing $C_{L,max}$ as was shown previously[4]. This behavior is clearly illustrated in Figs. 10 and 11. For the VR-7, $C_{L,max}$ is increased in the vicinity of the static-stall angle, and at the largest C_μ,

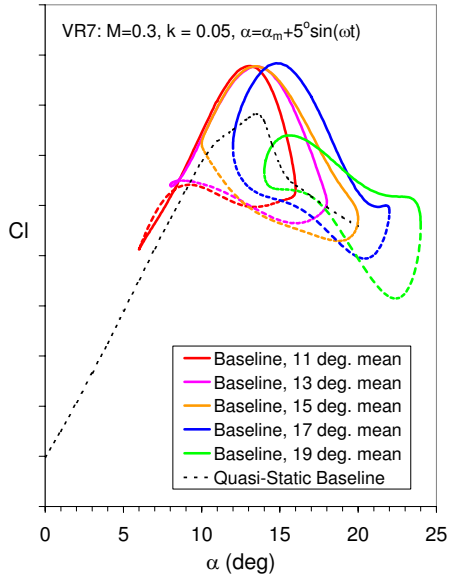

Figure 4. Unsteady lift coefficient for the baseline case for five different mean angles of attack (VR-7 airfoil).

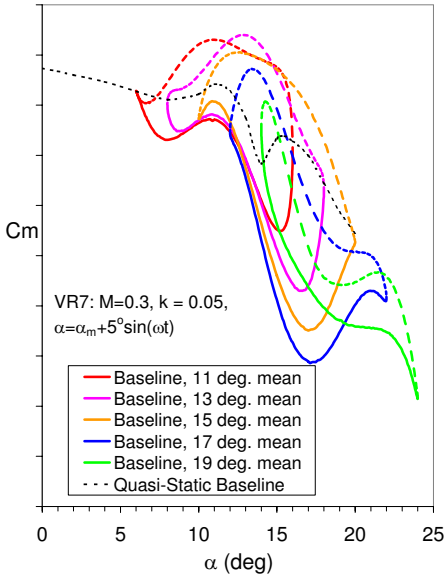

Figure 5. Unsteady pitching moment coefficient for the baseline case for five different mean angles of attack (VR-7 airfoil).

the improvement in $C_{L,max}$ over the baseline dynamic case is approximately 35%. Note, however, that the minimum moment associated with the baseline value is not materially affected by the forcing. In fact, it either remains unchanged, or is slightly increased. Moreover, the C_M excursions are consistently reduced with increasing C_μ. A significant challenge when applying control at high M is delivering enough amplitude from the slot to supply sufficient control authority. In order to maintain constant C_μ, the slot rms velocity must scale linearly with the free stream velocity; see Nagib et al.[7]for a detailed discussion of scaling of AFC. Because of limitation on the actuators, the C_μ produced in this investigation at $M > 0.3$ was therefore very low. Although control at $M = 0.35$ produced slightly more negative moments, the overall excursions are approximately the same. Increasing M from 0.35 to 0.4, under the same forcing conditions exhibited very little difference in the $C_{L,max}$ or moment excursions[4]. The results presented in our earlier paper[4] demonstrated that, for the VR-7 airfoil, the time histories of both lift and moment coefficients are affected in the same way regardless of M in the range 0.3 to 0.4. Thus, even though the small C_μ is incapable of exerting significant control authority, the time histories indicate that the effect of forcing is not diminished with increasing Mach number. Thus, comparing Figs. 5 and 7, described earlier, to the results presented in Nagib et al.[4] we see a definite improvement in the efficacy of control on C_M at $M = 0.3$ in the deep-stall regime.

Based only on the VR-7 results, where the airfoil exhibits trailing-edge separation, one may argue that in the case of airfoils with leading-edge separation behavior, the compressibility effects and possible existence of shocks may lead to a different

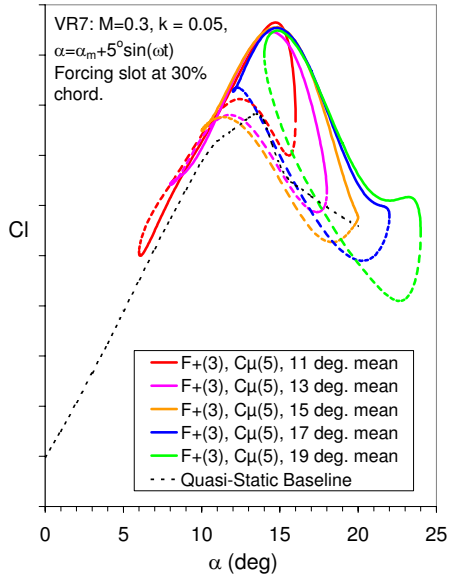

Figure 6. Unsteady lift coefficient with AFC for five different mean angles of attack (VR-7 airfoil).

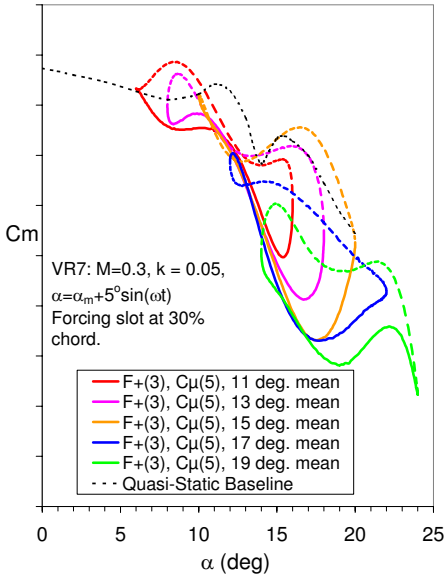

Figure 7. Unsteady pitching moment coefficient with AFC for five different mean angles of attack (VR-7 airfoil).

outcome. Here, we present for the first time clear evidence to the contrary using an extensive series of tests with the VR-22 model. Figures 12, 13, 14, and 15 display sample data for the VR-22 airfoil showing the effect of varying the mean incidence angle at $M = 0.3$, while maintaining incidence angle excursions of 5^o, for baseline (Figs. 12 and 13) and controlled (Figs. 14 and 15) cases. Comparing these figures to Figs. 4, 5, 6 and 7, we can see that the VR-22 airfoil not only has higher $C_{L,max}$ and $C_{M,min}$ values, but that the dynamic excursions in C_L and C_M are greater than for the VR-7. Figures 16 and 17 compare the effects of AFC on the VR-22 airfoil for $M = 0.3$ and $M = 0.35$. While the AFC did not significantly affect $C_{L,max}$ (most likely due to the low forcing amplitude as discussed earlier), it increased C_L substantially at post-stall alphas, and appreciably reduced the unsteady excursions in both C_L and C_M. The chordwise pressure distributions for the cases shown in Figs. 16 and 17 are presented for three different angles of attack in Fig. 18 ($\alpha = 16^o$ during pitch-up), Fig. 19 ($\alpha_{max} = 18^o$), and Fig. 20 ($\alpha = 16^o$ during pitch-down). In Fig. 18, both the baseline and AFC cases exhibit supercritical regions near the leading edge at both Mach numbers, and there is evidence of a shock around $x/c = 0.08$. This shock signature was not seen in subcritical cases at lower Mach numbers or at lower angles of attack. Figs. 19 and 20 clearly demonstrate the significant effects of the AFC on the leading-edge region in the presence of supercritical flow. In both these figures, the baseline cases at each Mach number are subcritical, but with AFC, the leading-edge suction peak grows substantially, resulting in supercritical conditions upstream of the AFC slot location (vertical dotted line). Therefore, these results demonstrate that AFC is not hindered by the

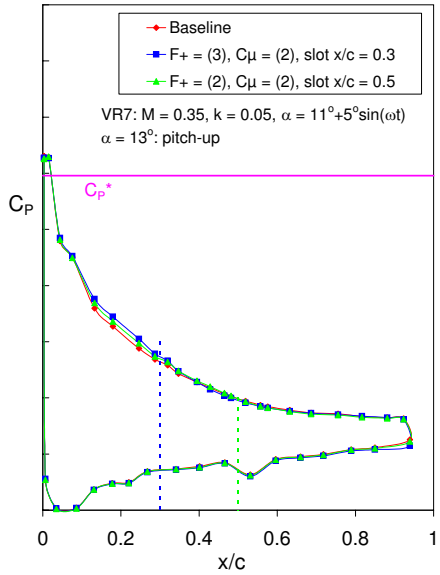

Figure 8. Chordwise pressure coefficient distributions for baseline and AFC cases for $M = 0.35$, $\alpha = 13^o$ during pitch-up (VR-7 airfoil).

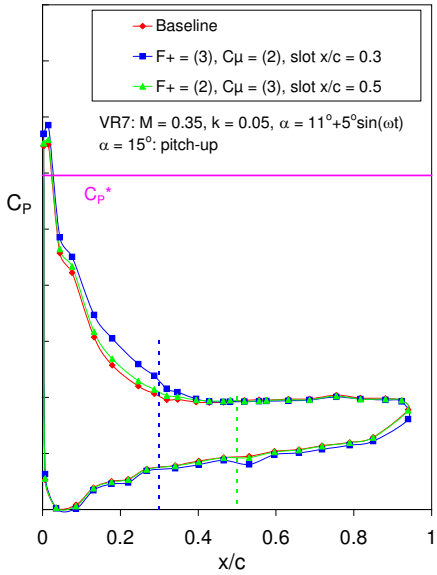

Figure 9. Chordwise pressure coefficient distributions for baseline and AFC cases for $M = 0.35$, $\alpha = 15^o$ during pitch-up (VR-7 airfoil).

presence of supercritical flow in the leading-edge region, and that the AFC is capable of enhancing airfoil performance in the deep-stall regime such that supercritical flow is induced. In the discussion to this point, only lift and moment coefficient results have been used to illustrate the AFC performance under compressible flow conditions. It is also of value to examine the effects of this control technique on the airfoil drag. Examples of instantaneous wake profiles, time-mean momentum deficit in the wake, and computed drag coefficient were given by Nagib et al.[4] for the light-stall case, and one case is shown in Fig. 21 of this paper. In general, the drag reduction is not large. This is mainly due to the relatively low excitation amplitudes (C_μ) available as the free-stream velocity increases.

The results suggest two possible observations that can be drawn from the present work. First, the effectiveness of control improves as the airfoil enters further into deep stall. Second, it appears that the efficacy of forcing diminished with increasing Mach number, as has been suggested by Carr and Chandrasekhara[6]. However, our results presented here clearly demonstrate that the main reason for the second (erroneous) observation is the reduction in the relative forcing amplitude[7]. It is clear from these results (see also Fig. 23 of Nagib et al.[4]) that for comparable values of the forcing amplitude, the lift enhancement is independent of Mach number over the range from 0.1 to 0.4. This is true for both the light-to-moderate stall conditions, where the lift enhancement monotonically increases up to approximately 10% improvement, and for the deep stall cases (19^o mean angle), where the lift enhancement can be by as much as 30%.

4. Conclusions

Pulsating zero-mass flux jets introduced from spanwise slots at various locations on the upper surface of oscillating VR-7 and VR-22 airfoil models are shown to be effective in controlling lift, moment and drag coefficients over the range of Mach numbers from 0.1 to 0.4. This control is demonstrated from light to deep stall conditions, for airfoils exhibiting either trailing-edge or leading-edge separation behavior. Even in presence of local shocks, maintaining the non-dimensional frequency and amplitude of the forcing unchanged, results in comparable modifications of the aerodynamic coefficients throughout this Mach number range. Contrary to the earlier speculations of Carr[5] and Carr and Chandrasekhara[6], it is clear that AFC techniques can be effective for at least some oscillating airfoils operating within the compressible regime. Their documented conclusions may only be valid for the particular airfoil used and the forcing conditions applied. Based on our results, it appears that active flow control techniques are only limited by their ability to generate the adequate forcing conditions at the higher Mach numbers required for applications such as rotorcraft, and we should encourage the design and development of actuators that can deliver the momentum required at the higher Mach numbers. Technologies leading to actuators that can be integrated into the rotorcraft blade, currently under development, should remain a high priority of the active flow-control field.

References

[1] GREENBLATT, D. AND WYGNANSKI, I.: "Parameters affecting dynamic stall control by oscillatory excitation". AIAA Paper 99-3121, 17th AIAA Applied Aerodynamics Conference, Norfolk, VA, USA (1999).

[2] MCALISTER, K. W., PUCCI, S. L., MCCROSKEY, W. J. AND CARR, L. W.: "An experimental study of dynamic stall on advanced airfoil sections. Volume 2. Pressure and force data". NASA TM 84245, (1982).

[3] GREENBLATT, D., KIEDAISCH, J. AND NAGIB, H.: "Unsteady-Pressure Corrections In Highly Attenuated Measurements At High Mach Numbers". AIAA 2001-2983, 31st AIAA Fluid Dynamics Conference & Exhibit, Anaheim, CA, USA (2001).

[4] NAGIB H., KIEDAISCH, J., GREENBLATT, D., WYGNANSKI, I, AND HASSAN, A.: "Effective Flow Control for Rotorcraft Applications at Flight Mach Numbers". AIAA 2001-2974, 31st AIAA Fluid Dynamics Conference & Exhibit, Anaheim, CA, USA (2001).

[5] CARR, L. W.: "Progress in the analysis and prediction of dynamic stall". AIAA Journal of Aircraft, Vol. 25, No. 1 (1988) pp. 6-17.

[6] CARR, L. W. AND CHANDRASEKHARA, M. S.: "Compressibility effects on dynamic stall". Progress in Aerospace Sciences, Vol. 32, (1996) pp. 523-573.

[7] NAGIB H., KIEDAISCH, J., REINHARD, P., and DEMANETT, B.: "Control Techniques for Flows with Large Separated Regions: A New Look at Scaling Parameters", AIAA Paper No. 2006-2857, 3rd AIAA Flow Control Conference, (2006).

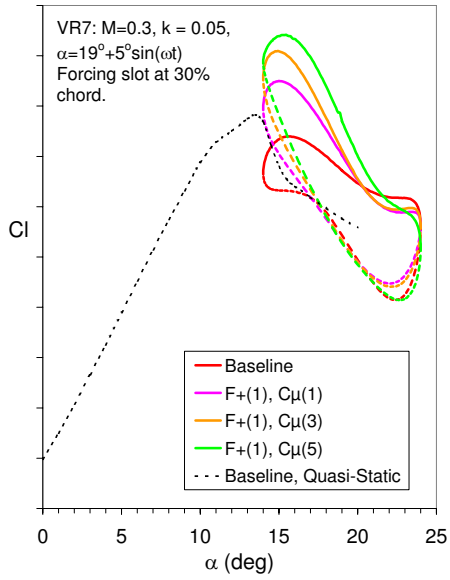

Figure 10. Unsteady lift coefficient for deep stall comparing different AFC amplitudes to baseline and quasi-steady cases (VR-7 airfoil).

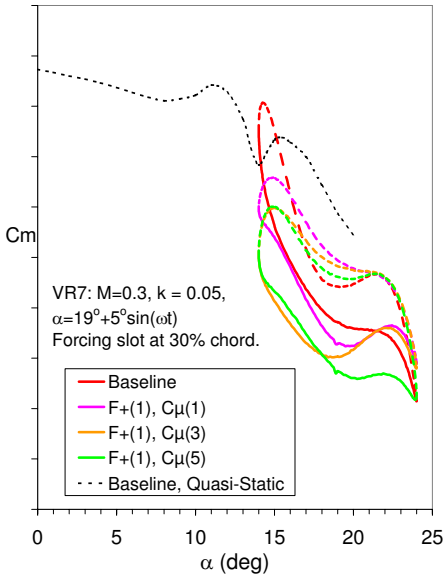

Figure 11. Unsteady pitching moment coefficient for deep stall comparing different AFC amplitudes to baseline and quasi-steady cases (VR-7 airfoil).

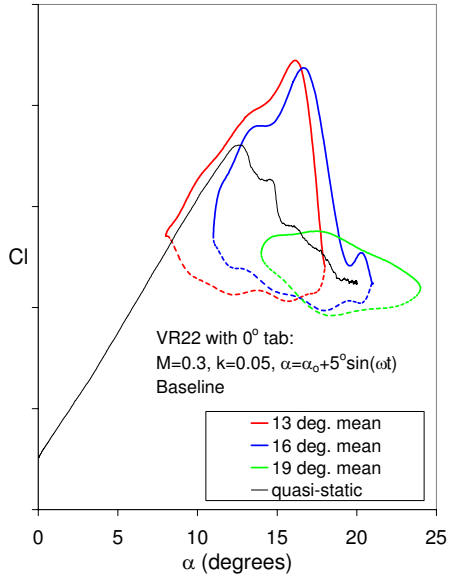

Figure 12. Unsteady lift coefficient for the baseline case for three different mean angles of attack (VR-22 airfoil).

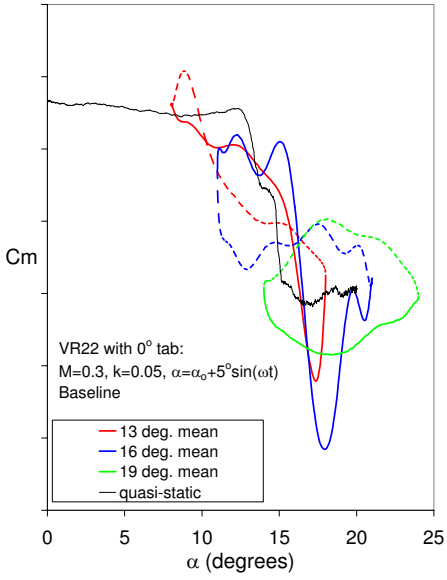

Figure 13. Unsteady pitching moment coefficient for the baseline case for three different mean angles of attack (VR-22 airfoil).

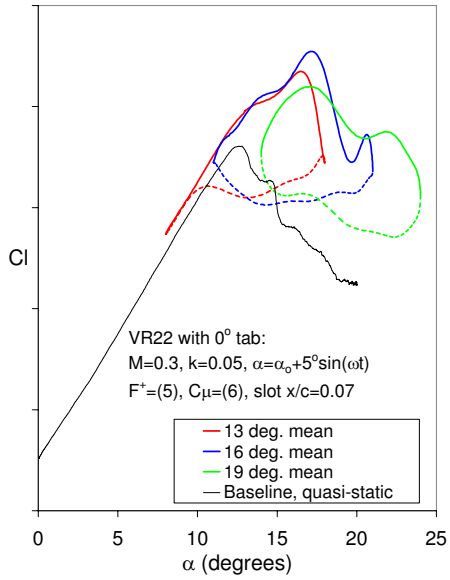

Figure 14. Unsteady lift coefficient with AFC for three different mean angles of attack (VR-22 airfoil).

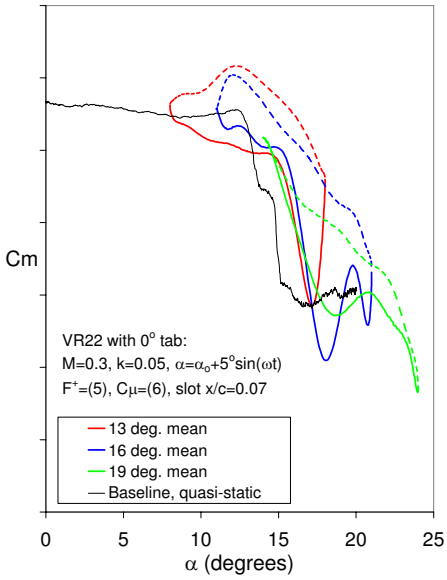

Figure 15. Unsteady pitching moment coefficient with AFC for three different mean angles of attack (VR-22 airfoil).

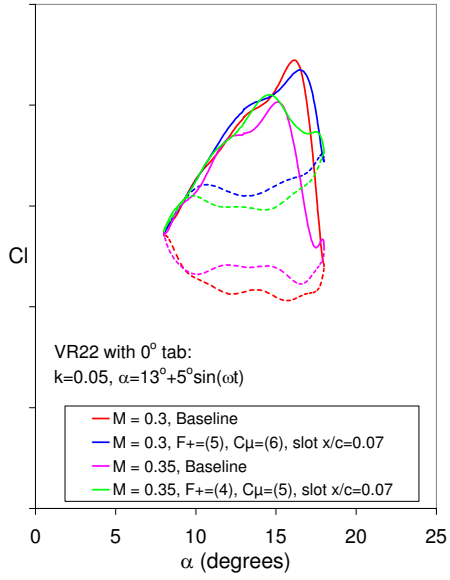

Figure 16. Unsteady lift coefficient comparing baseline and AFC cases for $M = 0.3$ and $M = 0.35$ (VR-22 airfoil).

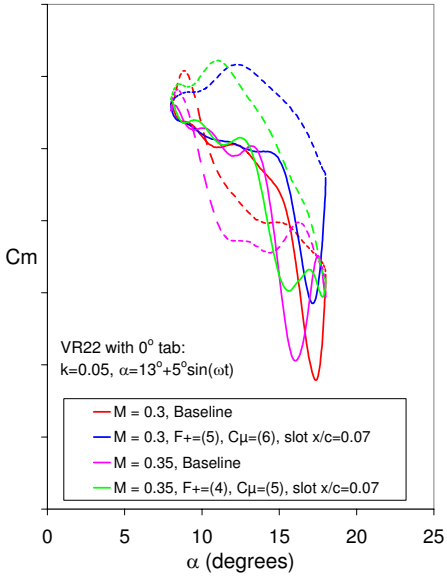

Figure 17. Unsteady pitching moment coefficient comparing baseline and AFC cases for $M = 0.3$ and $M = 0.35$ (VR-22 airfoil).

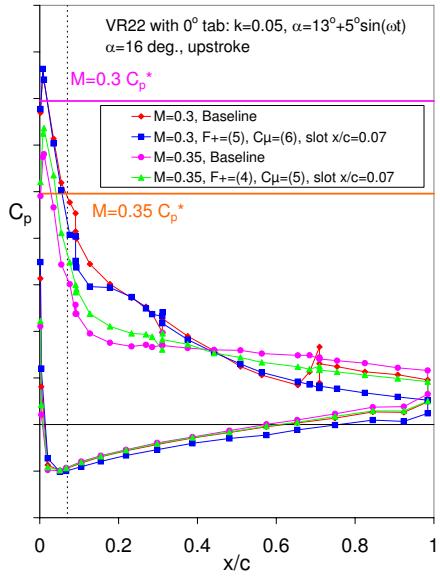

Figure 18. Chordwise pressure coefficient distributions for baseline and AFC cases for $M = 0.3$ and 0.35, $\alpha = 16^o$ during pitch-up (VR-22 airfoil).

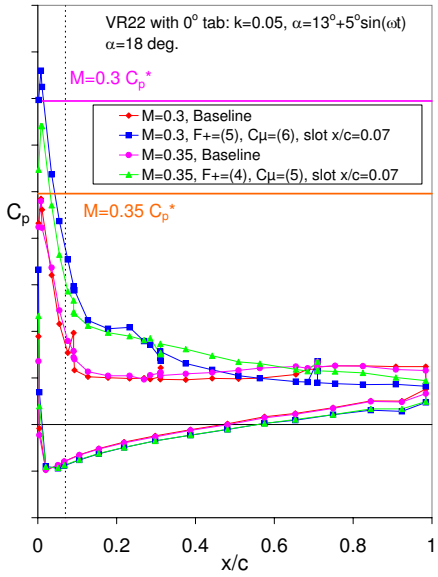

Figure 19. Chordwise pressure coefficient distributions for baseline and AFC cases for $M = 0.3$ and 0.35, $\alpha = 18^o$ during pitch-up (VR-22 airfoil).

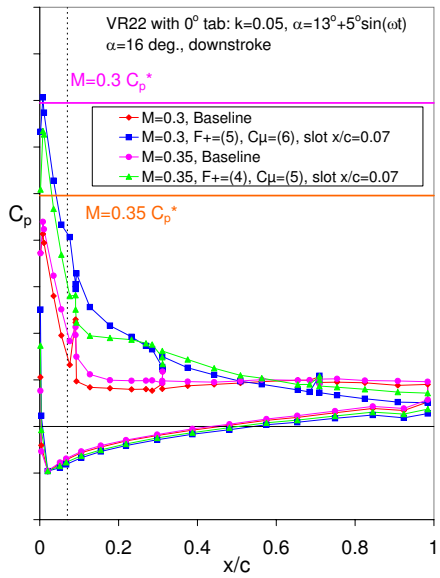

Figure 20. Chordwise pressure coefficient distributions for baseline and AFC cases for $M = 0.3$ and 0.35, $\alpha = 16^o$ during pitch-down (VR-22 airfoil).

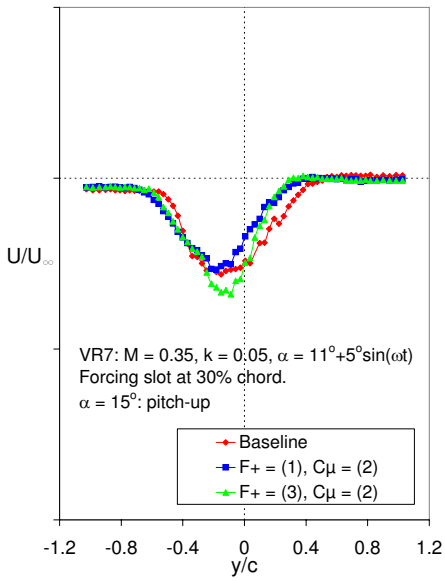

Figure 21. Normalized wake velocity profiles for baseline and AFC cases for $M = 0.35$, $\alpha = 15^o$ during pitch-up (VR-7 airfoil).